Title

A pore-expanded supramolecular organic framework and its enrichment of photosensitizers and catalysts for visible-light-induced hydrogen production

Journal

Organic Chemistry Frontiers, 6(10)

ISSN

2052-4110

Authors

Yan, Meng
Liu, Xu-Bo
Gao, Zhong-Zheng
et al.

Publication Date

2019-05-15

DOI

10.1039/c9qo00382g

Peer reviewed

A pore-expanded supramolecular organic framework and its enrichment of photosensitizers and catalysts for visible-induced hydrogen production

Meng Yan[1], Xu-Bo Liu[1], Zhong-Zheng Gao[1], Yi-Peng Wu[1], Hui Wang[1], Dan-Wei Zhang[1], Yi Liu[2*] & Zhan-Ting Li[2*]

[1]*Department of Chemistry, Collaborative Innovation Centre of Chemistry for Energy Materials (iChEM), and Shanghai Key Laboratory of Molecular Catalysis and Innovative Materials, Fudan University, 2205 Songhu Road, Shanghai 200438, China*

[2]*The Molecular Foundry, Lawrence Berkeley National Laboratory, One Cyclotron Road, Berkeley, California 94720, U.S.A.*

Received January 1, 2016; accepted February 2, 2016; published online March 3, 2016

A pore-expanded three-dimensional supramolecular organic framework **SOF-bpb**, with a previously unattained aperture size of 3.6 nm, has been constructed in water from the co-assembly of cucurbit[8]uril (CB[8]) and tetraphenylmethane-cored 1,4-bis(pyridin-4-yl)-benzene-appended building block **M1**. The periodicity of **SOF-bpb** in water and in the solid state has been confirmed by synchrotron X-ray scattering and diffraction experiments. **SOF-bpb** can adsorb anionic and neutral Ru^{2+} complex photosensitizers and anionic Wells-Dawson-type and Keggin-type polyoxometalates (POMs). The adsorption leads to important enrichment effect which remarkably increases the catalytic efficiency of the Ru^{2+} complex-POM systems for visible light-induced reduction of protons to produce H_2. The expanded aperture of **SOF-bpb** also increases the light transmittance of its solution and thus leads to enhanced photocatalytic activities as compared against the prototypical SOF that has an aperture size of 2.1 nm.

Supramolecular organic framework, large pore, photocatalysis, hydrogen production, porous material, cucurbit[8]uril

Citation: Yan M, Liu XB, Gao ZZ, Wu YP, Wang H, Zhang DW, Liu Y, Li ZT. A pore-expanded supramolecular organic framework and its enrichment of photosensitizers and catalysts for visible-induced hy-drogen production. *Sci China Chem*, 2019, 62: 1−2, doi: 10.1007/s11426-015-5408-0

1 Introduction

Three-dimensional (3D) porous materials with aperture sizes ranging from 1 to 10 nm have attracted a lot of attentions for their promising applications as adsorption, purification, catalysis and biomedical materials [1–3]. Large pores, with internal pore diameter being >3 nm, are not only synthetic challenges that are fundamentally important, but also in principle allow for inclusion of large organic, inorganic or even biological molecules [4]. Currently, a variety of two-dimensional frameworks of large pores have been constructed, which can stack to form deep channels [5]. However, attempts for the preparation of large pores from long tetrahedral or octahedral building blocks often yield interpenetrating structures of diamondoid or cubic topology as a result of strong stacking of the conjugated linkers [6].

We and others have developed the homogeneous self-assembly strategy for the generation of water-soluble supramolecular organic frameworks (SOFs) from multiarmed building blocks and cucurbit[8]uril (CB[8]) [7–15], which is driven by CB[8]-encapsulation-enhanced dimerization of appended pyridinium-derived aromatic units of the multiarmed monomers at room temperature [16]. The multicationic feature of the multiarmed monomers not only provide the resulting SOFs with good water-solubility, but also avoid interpenetration of the porous frameworks. We previously reported that 4-phenylpyridinium-appended tetrahedral monomers co-assemble with CB[8] to afford diamondoid SOFs that have a pore aperture of 2.1 nm [9].

*Corresponding authors (emails: ztli@fudan.edu.cn or yliu@lbl.gov)

We herein describe the self-assembly of a diamondoid SOF of 3.6 nm-aperture size from a 1,4-bis(pyridin-4-yl)benzene (BPB)-appended tetrahedral monomer and CB[8]. We further demonstrate that this expanded SOF is highly stable and able to simultaneously adsorb $[Ru(bpy)_3]^{2+}$-derived photosensitizers and polyoxametalate (POM) catalysts of very low concentrations, leading to enhanced efficiency of proton reduction when compared against the prototypical SOF of 2.1 nm-aperture size.

2 Results and discussion

Tetrahedral compound **M1** was used for the generation of the expanded 3D SOF. Within the cavity of CB[8], it was expected that fully eclipsed anti-parallel stacking of two BPB units would be disfavored due to the electrostatic repulsion of the pyridinium units (Figure 1) [17], instead a slipped anti-parallel stacking was expected, from which the formation of new expanded 3D framework would occur [18]. For the synthesis of **M1** (Scheme 1), compound **3** was prepared from the reaction of **1** [19] and **2** [20] in hot DMF, followed by treatment with an excess of methyl iodide in MeCN under reflux. After ion exchange, **M1** was obtained as a highly water-soluble chloride salt.

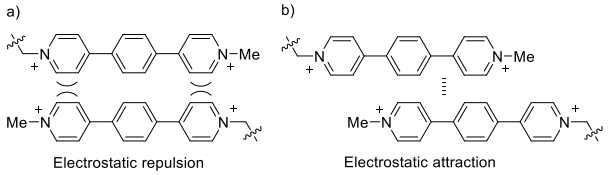

Figure 1 a) Unfavorable eclipsed anti-parallel stacking and b) favorable slipped anti-parallel stacking patterns of the BPB units of **M1**.

Octacationic salt **M1** was highly water-soluble (>4.0 mM), whereas CB[8] has a very low water-solubility (<20 μM) [21]. Mixing **M1** and CB[8] in a 1:2 molar ratio led to a homogeneous solution with the concentration of CB[8] being increased to > 2.0 mM. Similar remarkable solubilization has been observed for other reported SOFs and considered as an evidence for the formation of the framework structures. The ^{1}H NMR spectrum in D_2O showed poorly resolved peaks for both molecules (Figure S1), indicative of substantial complexation. Previous studies showed that, for tetrahedral monomers, the appended aromatic arms selectively form 2:1 complexation with CB[8], which corresponds to a 1:2 stoichiometry [9]. The encapsulation of the appended aromatic units by CB[8] typically caused pronounced hypochromism of the former. UV–vis titration experiments revealed an inflection point for this hypochromic effect at [CB[8]]/[**M1**] = 2.0 (Figure S2) when plotting the hypochromism of the maximum absorption (318 nm) of **M1** (1.0 mM) against [CB[8]], further confirming the 1:2 stoichiometry.

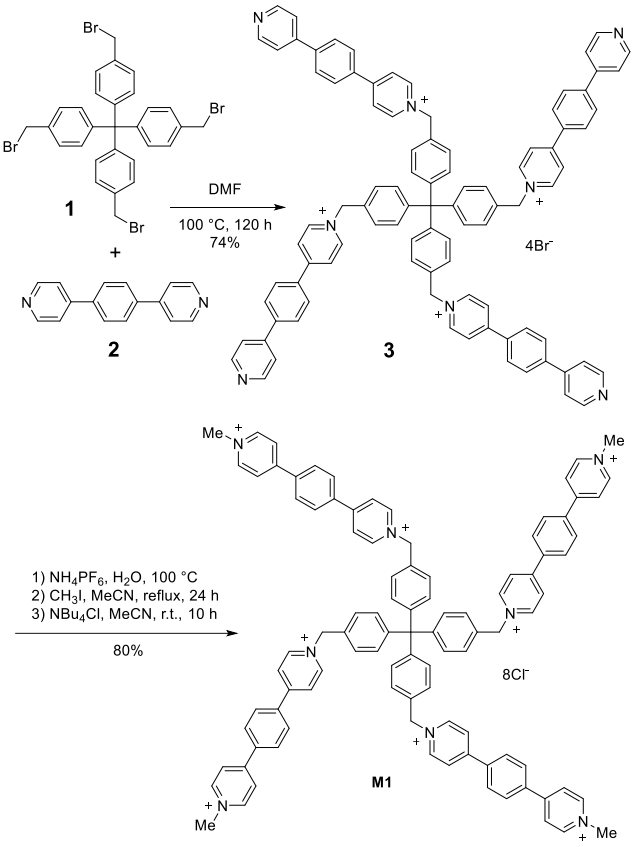

Scheme 1 The synthesis of compound **M1**.

Dynamic light scattering (DLS) experiments revealed the formation of large aggregates in the 1:2 solution of **M1** (1.0 mM) and CB[8] in water and the hydrodynamic diameter (D_H) of the aggregates was determined to be 94.4 nm (Figure S3a). Upon diluting the solution to [**M1**] = 0.03 mM, the 1:2 solution still formed aggregates of D_H = 37.3 nm. In the absence of CB[8], DLS measurement afforded a D_H of 3.7 nm for the solution of **M1** (0.1 mM), reflecting significantly weaker aggregation (Figure S3b).

Isothermal titration calorimetry (ITC) experiments were conducted by gradually adding **M1** to the aqueous solution of CB[8] (Figure S4), from which the apparent association constant K_a for the 2:1 complexes between the BPB units of **M1** and CB[8] was determined to be 1.5×10^{10} M^{-2}, which was notably lower than that of the prototypical SOF with shorter 4-phenylpyridinium binding moiety, but still enabled the formation of a stable expanded SOF (vide infra, Figure 3). The associated enthalpic (ΔH) and entropic (-TΔS) contributions were -171.54 and 27.07 kJ mol^{-1}, respectively, indicating that the co-assembly was driven enthalpically and unfavorably by entropy.

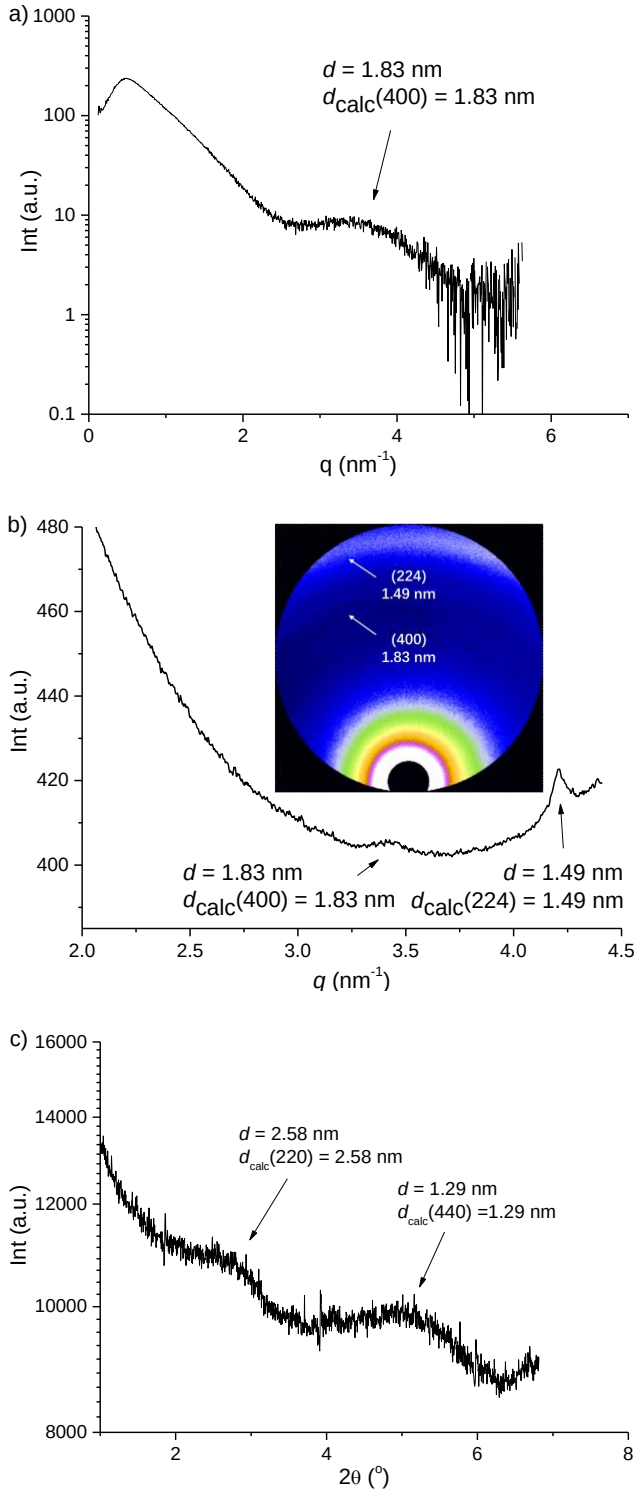

Figure 2 a) Solution-phase synchrotron SAXS profile of **SOF-bpb** ([**M1**] = 2.0 mM). b) Solid-phase synchrotron SAXS profile of **SOF-bpb**, inset: 2D profile. c) Solid-phase synchrotron XRD profile of **SOF-bpb**.

Synchrotron small angle X-ray scattering (SAXS) profile for the 1:2 solution of **M1** (2.0 mM) and CB[8] revealed a discernible broad peak with the d-spacing centered around 1.83 nm (Figure 2a). This peak matched with the calculated {400} spacing (1.83 nm) of the modelled network obtained using previously describe method [23], supporting the formation of a new periodic water-soluble supramolecular organic framework, which we named as **SOF-bpb** to reflect the use of BPB as the appended binding unit (Figure 3). The synchrotron SAXS profile of **SOF-bpb** microcrystals, obtained by slow evaporation of the above solution at room temperature, displayed two relatively sharper peaks centered at 1.83 and 1.49 nm (Figures 2b), respectively, which can be assigned to the {400} and {224} facets of the modeled structure of **SOF-bpb**. The peaks were also observed on the two-dimensional synchrotron SAXS profile (Figures 2b, inset). Synchrotron X-ray diffraction (XRD) profile of the microcrystals revealed discernible peaks with the d-spacing centered around 2.58 and 1.29 nm (Figure 2c). The peaks matched well with the calculated {220} and {440} spacing of the modelled network. These results supported that **SOF-bpb** also maintained the ordered porosity in the solid state. Thermogravimetric analysis showed that the **SOF-bpb** microcrystals were stable at ≤ 370 °C (Figure S5). The transmission electron microscopic (TEM) image showed a uniform bulk morphology, whereas elemental mapping analysis confirmed the compositions of the C, N, O and Cl elements (Figure S6a).

The modeled structure of **SOF-bpb** revealed a diamondoid framework pattern. The pore aperture, which was defined by six CB[8] units in one cyclohexane-like self-assembled macrocycle, was estimated to be about 3.6 nm (Figure 3a), which was the largest among the reported diamondoid-type SOFs [8d,e,9]. The modelled structure of **SOF-bpb**, including the chloride anions, has approximately 85% of void volume, which is also notably larger than that (77%) of the prototypical SOFs that bear the 4-phenylpyridinium binding unit [9].

The ability of **SOF-bpb** for the adsorption or enrichment of photosensitizers ($[Ru(bdc)_3]^{4-}$ as K^+ salt and $(Ru(bpy)_2(bdc))$ (Figure 3b), POM catalysts (Wells-Dawson (WD)-type POM ($[P_2W_{18}O_{62}]^{6-}$ as K^+ salt and Keggin (K)-type POM ($[PW_{12}O_{40}]^{3-}$ as Na^+ salt) or their four mixtures ($K_4Ru(bdc)_3$/WD-POM (10:1), $K_4Ru(bdc)_3$/K-POM (10:1), $Ru(BPY)_2(bdc)$/WD-POM (10:1) and $Ru(bpy)_2(bdc)$/K-POM (10:1)) was then investigated in water by using the fluorescence spectroscopy. All these molecular species have a size of 1.1-1.3 nm. The combination of the ruthenium complex and the polyoxometalate can constitute an integrated photocatalytic system for visible light-induced proton reduction to produce hydrogen [8e,f,24]. It was found that all these species quenched the fluorescence of **SOF-bpb** in water. Titration experiments indicated that maximum quenching was reached after about 1.6, 1.5, 1.4, and 1.8 equiv. of the four single-component species (relative to [**M1**] in **SOF-bpb**) were added. The values corresponded to a relative ratio of 0.80, 0.38, 1.0 and 0.68 for their anion concentration over the concentration of **M1** (10 μM) (Figures S7–S10). Addition of the $K_4Ru(bdc)_3$/WD-POM

(10:1), Ru(bpy)$_2$(bdc)/WD-POM (10:1), Ru(bpy)$_2$(bdc)/K-POM (10:1) or K$_4$Ru(bdc)$_3$/K- POM (10:1) mixtures into the solution of **SOF-bpb** also quenched the fluorescence to a comparable extent as the pure Ru^{2+} complex (Figure S11-S14). In contrast, when adding either of the above guests or their mixtures to the solution of **M1**, fluorescence quenching was considerably less effective, highlighting the enriching effect of the **SOF-bpb** framework. This adsorption for anionic species has been rationalized by the formation of soft acid (pyridinium cation of BPB)-soft base (Ru^{2+} complexes or POMs) ion pairs and hard acid (Na^+ or K^+)-hard base (Cl^-) ion pairs [8c]. The adsorption of **SOF-bpb** for zwitterionic complex Ru(bpy)$_2$(bdc) might be attributed to that the steric $[Ru(bpy)_3]^{2+}$ could not form efficienct ion-pair interactions. As a result, the zwitterion could behave formally as a dianionic soft base. The above 10:1 ratio of the Ru^{2+} complexes/POM mixture was adapted from a related, previously optimized catalytic system that shows good catalytic activities for visible light-induced water reduction to hydrogen [8e,f].

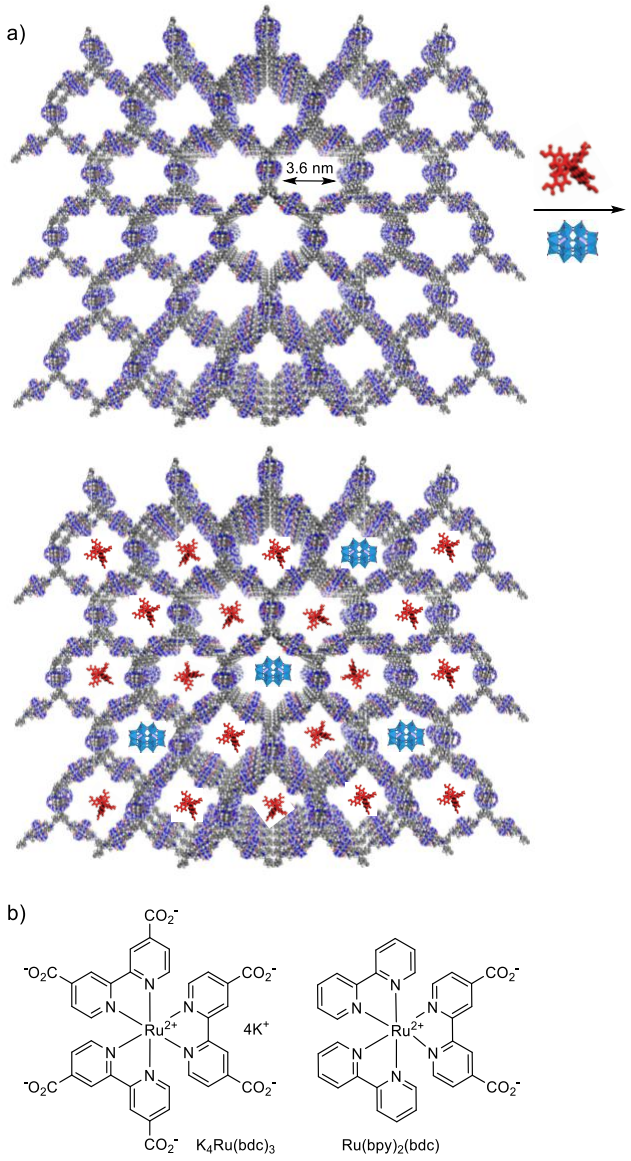

Figure 3 a) Modelled porous structure of **SOF-bpb** and simultaneous adsorption of Ru-photosensitizer (red) and polyoxometallate catalyst (indigo). b) Structural formulas of K$_4$Ru(bdc)$_3$ and Ru(bpy)$_2$(bdc)).

DLS revealed that, after adsorption of the ruthenium complexes and the POM salts, the four investigated **SOF-bpb** solutions afforded a D_H value that was comparable with that (53 nm) of the pure sample (Figures S3b and S15), indicating that its porosity regularity was maintained after adsorption and no significant aggregation took place. Slow evaporation of the solution of **SOF-bpb** ([**M1**] = 0.1 mM), K$_4$[Ru(bdc)$_3$] (20 μM) and WD-POM (2 μM) afforded red solid powders. Elemental mapping analysis for the microcrystals confirmed the compositions of the C, N, O, Ru, Cl, W and P elements (Figure S6b).

Table 1 Enhanced hydrogen evolution in the solution of **SOF-bpb** in water and methanol (4:1, v/v, pH = 1.8 with HCl) containing Ru^{2+} complex photosensitizers and POM catalysts [a)]

Entry	[**M1**] (mM)	Ru^{2+} (μM)	POM (μM)	**TON-1** [f)]	**TON-2** [g)]	**TON-1 /TON-2**
1	0.1	A (20)	C (0)	0	0	-
2	0.1	A (0)	C (2.0)	0	0	-
3	0.1	B (20)	D (0)	0	0	-
4	0.1	A [b)] (2.0)	C [d)] (0.2)	781	0	-
5	0.1	A (6.0)	C (0.6)	763	15	51
6	0.1	A (10)	C (1.0)	429	26	17
7	0.1	A (16)	C (1.6)	475	51	9
8	0.1	A (20)	C (2.0)	505	49	10
9	0.1	A (26)	C (2.6)	367	41	9
10	0.1	A (30)	C (3.0)	316	37	9
11	0.01	A (20)	C (2.0)	117	49	3
12	0.05	A (20)	C (2.0)	257	49	5
13	0.1	A (20)	C (2.0)	352	49	7
14	0.15	A (20)	C (2.0)	272	49	6
15	0.2	A (20)	C (2.0)	246	49	5
16	0.1	A (20)	D [e)] (2.0)	634	43	15
17	0.1	B [c)] (20)	C (2.0)	608	45	14
18	0.1	B (20)	D (2.0)	599	38	16

a) Irradiation time = 20 h, b) A = K$_4$Ru(bdc)$_3$, c) B = Ru(bpy)$_2$(bdc), d) C = Wells-Dawson-type POM, e) D = Keggin-type POM, f) in the presence of **SOF-bpb**, and g) without **SOF-bpb**.

Visible light (>410 nm)-induced proton reduction to produce H_2 in ruthenium complex and POM-contained **SOF-bpb** solution in diluted hydrochloric water (pH = 1.8) was then investigated. DLS experiment revealed that **SOF-bpb** was stable in this acidic medium after irradiation of long time (20 h) (Figures S3b and S15). The reactions were conducted by irradiating an 2-mL water-methanol (4:1, v/v) solution of **SOF-bpb** in the presence of different amounts of K$_4$[Ru(BDC)$_3$] and WD-POM, the molar ratio of which was kept at 10:1 (Table 1), in a sealed 5-mL glass

bottle. Methanol was used as sacrificial electron donor in this study. Both the ruthenium complex and POM sample were indispensable for the reduction of proton (entries 1-3, Table 1). Under all studied conditions, **SOF-bpb** exhibited remarkable enhancement effect (up to 51-fold, entry 5, Table 1) for the catalytic activity (entries 4-18, Table 1), which can be rationally attributed to its enrichment for the species and thus the increase of their effective concentration in the interior of **SOF-bpb**. This promotion effect became increasingly prominent at lowered concentrations (entries 4-10, Table 1). In particular, at the lowest concentration ([$K_4Ru(bdc)_3$] = 2.0 μM and [WD-POM] = 0.2 μM), in the absence of **SOF-bpb**, no H_2 evolution was observed. However, with the promotion of **SOF-bpb** through the enrichment of both species, the turnover number (TON) for H_2 production reached the highest value of 781 (defined as n(1/2H_2)/n(POM) (entry 4, Table 1). This value corresponded to a H_2 evolution rate, that is, turnover frequency (TOF), of 7079 μmol/g·h (based on POM), which was about two times of the highest TON achieved by the prototypical SOF that bears the short 4-phenylpyridinium binding moiety under similar conditions [9]. This increased catalytic efficiency of ([$Ru(bdc)_3$]$^{4+}$/WD-POM)@**MOF-bpb** system may be attributed to the higher light transmittance of its larger pores. At [$Ru(bdc)_3$] = 20 μM and [WD-POM] = 2 μM, gradient experiments revealed (entries 11-15, Table 1) that, at [**M1**] = 0.1 mM, **SOF-bpb** caused the highest TON, which decreased notably at higher concentration of the framework, which may be ascribed to the decrease of light transmittance of the solution. At [**M1**] = 0.1 mM, **SOF-bpb** also enhanced the catalytic efficiency of the $K_4Ru(bdc)_3$/K-POM, $Ru(BPY)_2(bdc)$/WD-POM and $Ru(bpy)_2(bdc)$/K-POM combinations (entries 16-18) and the related TON values were even higher than that of the $K_4Ru(bdc)_3$/WD-POM combination.

Table 2 Hydrogen evolution in the solution of **SOF-bpb** (0.1 mM) in water and methanol (4:1, v/v, pH = 1.8 with HCl) containing $K_4Ru(bdc)_3$ (20 μM) and WD-POM (2.0 μM) a)

Entry	TON-1	TON-2 b)	TON-1/TON-2
1	506	49	-
2	499	32	-
3	475	25	-
4	400	13	-
5	396	-	-
6	362	-	-
7	312	-	-
8	272	-	-
9	258	-	-
10	225	-	-

a) Irradiation time = 20 h, b) without **SOF-bpb**.

Irradiating the solution for longer time (20-70 hours) still led to H_2 evolution, even though the efficiency became increasingly lower (Figure S16). When the solution was left to stand for some time, typically 12 hours, the catalytic activity of the system recovered to a considerable extent. In this way, the solution could be irradiated for ten times (Table 2) to produce H_2, albeit with a decreasing efficiency. Control experiments showed that, in the absence of **SOF-bpb**, irradiating the solution of $K_4[Ru(BDC)_3]$ and WD-POM could also produce H_2 and this process could be conducted for four times after repeated standing. However, the catalytic efficiency was generally substantially lower (entries 1-4, Table 2). These results not only confirmed the enrichment effect of SOF-bpb, but also suggested that the enrichment increased the efficiency and stability of the bi-component catalytic system, which might be attributed to the fact that adsorption could decrease the aggregation of the photosensitizer and catalyst molecules [25]. DLS experiment for the SOF-bpb solutions after long time and repeated irradiation afforded D_H that was comparable to that of the originally prepared sample (Figure S15), supporting that the frameworks still maintained their integrity to enable continued enrichment effect.

3 Conclusions

We have demonstrated the construction of a 3.6 nm-aperture 3D SOF by elongating the peripheral aromatic binding moiety of the tetrahedral building block. The new pore-expanded SOF exhibits very strong adsorption ability for Ru^{2+} complex photosensitizers and POM, which remarkably promotes their visible light-initiated photocatalysis for the proton reduction to produce hydrogen. The new SOF is highly stable to allow for repeated use and more transparent to allow for increased light transmittance and catalysis efficiency as compared with that of the prototypical SOF of smaller pore size. The good water-solubility and high stability of this 3.6 nm-aperture SOF bodes well for the generation of SOFs that possess even larger aperture for the encapsulation and delivery of biomacromolecules.

Acknowledgments This work was supported by National Natural Science Foundation of China (21432004, 21529201 and 21890732). Yi Liu thanks the support from the Molecular Foundry, a national user facility supported by the Office of Science, Office of Basic Energy Sciences, of the U.S. Department of Energy under Contract No. DE-AC02-05CH11231. We also thank Shanghai Synchrotron Radiation Facility (beamlines BL16B1 and BL14B1) for providing the beam time. Solution SAXS studies were conducted at the SIBYLS Beamline 12.3.1 of the Advanced Light Source (ALS), a national user facility supported by Department of Energy, Office of Basic Energy Sciences, through the Integrated Diffraction Analysis Technologies (IDAT) program, supported by DOE Office of Biological and Environmental Research. Additional support comes from the National Institute of Health project ALS-ENABLE (P30 GM124169) and a High-End Instrumentation Grant S10OD018483.

Conflict of interest The authors declare that they have no conflict of interest.

Supporting information The supporting information is available online at http://chem.scichina.com and http://link.springer.com/journal/11426.

1 Liu P, Chen GF. Eds. *Porous Materials: Processing and Applications*. Oxford: Butterworth-Heinemann Publisher, 2014
2 MacGillivray LR, Lukehart CM. Eds. *Metal-Organic Framework Materials*. Chichester: John Wiley & Sons, 2015
3 Zhu G, Ren H. Eds. *Porous Organic Frameworks: Design, Synthesis and Their Advanced Applications*. Berlin: Springer-Verlag, 2015
4 (a) Ma L, Falkowski JM, Abney C, Lin W. Nat Chem, 2010, 2: 838–846; (b) Wu MX, Yang YW. Chin Chem Lett, 2017, 28: 1135–1143; (c) Liu G, Sheng J, Zhao Y. Sci China Chem, 2017, 60: 1015–1022; (d) Yang T, Cui Y, Chen H, Li W. Huaxue Xuebao, 2017, 75: 339–350; (e) Cao L, Wang T, Wang C. Chin J Chem, 2018, 36: 754–764; (e) Liu D, Zou D, Zhu H, Zhang J. Small, 2018, 14: 1801454; (f) Yuan F, Tan J, Guo J. Sci China Chem, 2018, 61: 143–152; (g) Song Y, Sun Q, Aguila B, Ma S. Adv Sci, 2019, 6: 1801410; (h) Zhao X, Zhang Z, Cai X, Ding B, Sun C, Liu G, Hu C, Shao S, Pang M. ACS Appl Mater Interf, 2019, 11: 7884–7892
5 (a) Deng H, Grunder S, Cordova KE, Valente C, Furukawa H, Hmadeh M, Gándara F, Whalley AC, Liu Z, Asahina S, Kazumori H, O'Keeffe M, Terasaki O, Stoddart JF, Yaghi OM. Science, 2012, 366: 1018–1023; (b) Jin S, Furukawa K, Addicoat M, Chen L, Takahashi S, Irle S, Nakamura T, Jiang D, Chem Sci, 2013, 4: 4505–4511; (c) Fang Q, Zhuang Z, Gu S, Kaspar RB, Zheng J, Wang J, Qiu S, Yan Y. Nat Commun, 2014, 5: 4503; (d) Yang H, Du Y, Wan S, Trahan GD, Jin Y, Zhang W. Chem Sci, 2015, 6: 4049–4053; (e) Zhang Y, Zhan TG, Zhou TY, Qi QY, Xu XN, Zhao X. Chem Commun, 2016, 52: 7588–7591; (f) Zhang L, Jia Y, Wang H, Zhang DW, Zhang Q, Liu Y, Li ZT. Polym Chem, 2016, 7: 1861–1865
6 (a) Song BQ, Wang XL, Yang GS, Wang HN, Liang J, Shao KZ, Su ZM. CrystEngComm, 2014, 16: 6882–6888; (b) Tseng TW, Luo TT, Tsai CC, Lu KL. CrystEngComm, 2015, 17: 2935–2939; (c) Liao H, Wang H, Ding H, Meng X, Xu H, Wang B, Ai X, Wang C. J Mater Chem, A 2016, 4: 7416–7421; (d) Frank M, Johnstone MD, Clever GH. Chem Eur J, 2016, 22: 14104–14125; (e) Lin G, Ding H, Chen R, Peng Z, Wang B, Wang C, J Am Chem Soc, 2017, 139: 8705–8709; (f) Sheng D, Zhu L, Xu C, Xiao C, Wang Y, Wang Y, Chen L, Diwu J, Chen J, Chai Z, Albrecht-Schmitt TE, Wang S. Environ Sci Technol, 2017, 51: 3471–3479; (g) Ma T, Kapustin EA, Yin SX, Liang L, Zhou Z, Niu J, Li LH, Wang Y, Su J, Li J, Wang X, Wang WD, Wang W, Sun J, Yaghi OM. Science, 2018, 361: 48–52; (h) Ding H, Xie G, Lin G, Chen R, Peng Z, Yang C, Wang B, Wang C, Li J, Sun J. Nat Commun, 2018, 9: 5234
7 (a) Tian J, Wang H, Zhang DW, Liu Y, Li ZT. Natl Sci Rev, 2017, 4: 426–436; (b) Chen Y, Huang F, Li ZT, Liu Y. Sci China Chem, 2018, 61: 979–992; ()
8 (a) Zhang KD, Tian J, Hanifi D, Zhang Y, Sue ACH, Zhou TY, Zhang L, Zhao X, Liu Y, Li ZT. J Am Chem Soc, 2013, 135: 17913–17918; (b) Zhang L, Zhou TY, Tian J, Wang H, Zhang DW, Zhao X, Liu Y, Li ZT. Polym Chem, 2014, 5: 4715–4721; (c) Tian J, Xu ZY, Zhang, D.-W.; Wang, H.; Xie, S.-H.; Xu, D.-W.; Ren, Y.-H.; Wang, H.; Liu, Y.; Li, Z.-T. Nat Commun, 2016, 7, 11580; (d) Wu YP, Yang B, Tian J, Yu SB, Wang H, Zhang DW, Liu Y, Li ZT. Chem Commun, 2017, 53: 13367–13370; (e) Yu SB, Qi Q, Yang B, Wang H, Zhang DW, Liu Y, Li ZT. Small, 2018, 14: 1801037; (f) Li XF, Yu SB, Yang B, Tian J, Wang H, Zhang DW, Liu Y, Li ZT. Sci China Chem, 2018, 61: 830–835
9 (a) Tian J, Zhou TY, Zhang SC, Xie SH, Zhang DW, Zhao X, Liu Y, Li ZT. Nat Commun, 2014, 5, 5574; (b) Tian, J.; Yao, C.; Yang, W.-L.; Zhang, L.; Zhang, D.-W.; Wang, H.; Zhang, F.; Liu, Y.; Li, Z.-T. Chin Chem Lett, 2017, 28, 798–806
10 (a) Xu SQ, Zhang X, Nie CB, Pang ZF, Xu XN, Zhao X. Chem Commun, 2015, 51: 16417–16420; (b) Jiang SY, Zhao X. Chin J Polym Sci, 2019, 37: 1–10
11 Pfeffermann M, Dong R, Graf R, Zajaczkowski W, Gorelik T, Pisula W, Narita A, Müllen K, Feng X. J Am Chem Soc, 2015, 137: 14525–14532
12 Li Y, Dong Y, Miao X, Ren Y, Zhang B, Wang P, Yu Y, Li B, Isaacs L, Cao L. Angew Chem Int Ed, 2018, 57: 729–733
13 Lee HJ, Kim HJ, Lee EC, Kim J, Park SY. Chem Asian J, 2018, 13: 390–394
14 Madasamy K, Shanmugam VM, Velayutham D, Kathiresan M, Madasamy K, Velayutham D, Kathiresan M. Sci Rep, 2018, 8: 1354
15 Liu H, Zhang Z, Zhao Y, Zhou Y, Xue B, Han Y, Wang Y, Mu X, Zang S, Zhou X, Li Z. J Mater Chem, B 2019, 7: 1435–1441
16 (a) Ko YH, Kim E, Hwang I, Kim K. Chem Commun, 2007, 1305–1315; (c) Liu Y, Yang H, Wang Z, Zhang X. Chem Asian J, 2013, 8: 1626–1632; (c) Tian J, Zhang L, Wang H, Zhang DW, Li ZT. Supramol Chem, 2016, 28: 769–783; (d) Tian T, Chen L, Zhang DW, Liu Y, Li ZT. Chem Commun, 2016, 52: 6351–6362; (e) Wang R, Qiao S, Zhao L, Hou C, Li X, Liu Y, Luo Q, Xu J, Li H, Liu J. Chem Commun, 2017, 53: 10532–10535; (f) Wu S, Li J, Liang H, Wang L, Chen X, Jin G, Xu X, Yang HH. Sci China Chem 2017, 60: 628–634; (g) Yin ZJ, Wu ZQ, Lin F, Qi QY, Xu XN, Zhao X. Chin Chem Lett, 2017, 28: 1167–1171; (h) Zou H, Liu J, Li Y, Li X, Wang X, Small, 2018, 14, 1802234
17 Yang B, Yu SB, Wang H, Zhang DW, Li ZT. Chem Asian J, 2018, 13: 1312–1317
18 Zhang Y, Zhou TY, Zhang KD, Dai JL, Zhu YY, Zhao X. Chem Asian J, 2014, 9: 1530–1534
19 Tian J, Ding YD, Zhou TY, Zhang KD, Zhao X, Wang H, Zhang DW, Liu Y, Li ZT. Chem Eur J, 2014, 20: 575–584
20 Su YS, Chen CF. Org Lett, 2010 12: 1888–1891
21 Lagona J, Mukhopadhyay P, Chakrabarti S, Isaacs L. Angew Chem Int Ed, 2005, 44: 4844–4870
22 (a) Heitmann LM, Taylor AB, Hart PJ, Urbach AR. J Am Chem Soc, 2006, 128: 12574–12581; (b) Huang Z, Yang L, Liu Y, Wang Z, Scherman OA, Zhang X. Angew Chem Int Ed, 2014, 53: 5351–5355
23 Accelrys Materials Studio Release Notes, Release 7.0, Accelrys Software Inc., San Diego, USA, 2013 (accessed: December 2013) https://www.scientific-computing.com/press-releases/accelrys-materials-studio-70
24 (a) Sivakumar R, Thomas J, Yoon M. J. Photochem Photobiol C, 2012, 13: 277–298; (b) Lv H, Song J, Zhu H, Geletii YV, Bacsa J, Zhao C, Lian T, Musaev DG, Hill CL. J Catal, 2013, 307: 48–54; (c) Zhang ZM, Zhang T, Wang C, Lin Z, Long LS, Lin W. J Am Chem Soc, 2015, 137: 3197–3200.
25 (a) Mori K, Hara T, Mizugaki T, Ebitani K, Kaneda K. J Am Chem Soc, 2004, 126: 10657–10666; (b) Gan W, Dyson PJ, Laurenczy G. ChemCatChem, 2013, 5: 3124–3130; (c) Astruc D, Lu F, Aranzaes JR. Angew Chem Int Ed, 2005, 44: 7852–7872.

Table of Contents graphic